On the existence of chaotic circumferential waves in spinning disks

Arzhang Angoshtari[a] and Mir Abbas Jalali[b]
Center of Excellence in Design, Robotics and Automation, Department of Mechanical Engineering, Sharif University of Technology, P.O. Box 11365-9567, Azadi Avenue, Tehran, Iran

(Received 17 October 2006; accepted 10 April 2007; published online 11 June 2007)

We use a third-order perturbation theory and Melnikov's method to prove the existence of chaos in spinning circular disks subject to a lateral point load. We show that the emergence of transverse homoclinic and heteroclinic points lead, respectively, to a random reversal in the traveling direction of circumferential waves and a random phase shift of magnitude π for both forward and backward wave components. These long-term phenomena occur in imperfect low-speed disks sufficiently far from fundamental resonances. © *2007 American Institute of Physics*. [DOI: 10.1063/1.2735813]

Transversal vibration modes of hard disk drives (HDDs) are excited by the lateral aerodynamic force of the magnetic head. Previous work[1,2] has revealed that chaotic orbits are inevitable ingredients of phase space flows when the lateral force is large, or the disk is rotating near the critical resonant speed. For low-speed disks, however, an adiabatic invariant (a first integral) was found[2] using a first-order averaging based on canonical Lie transforms. According to the first-order theory, regular vibrating modes of imperfect, low-speed disks are independent of the angular velocity of the disk; i.e., Ω_0. In such a circumstance, the speed of circumferential waves is the natural frequency ω of the lateral mode derived from linear vibration analysis. HDDs are usually operated with angular velocities smaller than ω (safely below resonance). Moreover, the magnitude of the lateral force F is very small. Given these conditions, we show that it is impossible to continue the Lie perturbation scheme[2] up to terms of arbitrary order and remove the time variable t from the Hamiltonian. In fact, due to the special forms of nonlinearities in the dynamical equations of spinning disks, one cannot remove t from third-order terms. Subsequent application of a second-order Melnikov theory reveals that transverse homoclinic and heteroclinic points do exist for all $F,\Omega_0 \neq 0$. This implies chaos, or equivalently, nonintegrability of governing equations.

I. INTRODUCTION

Dynamics of continuum media, such as fluids, rods, plates, and shells, is usually formulated as a system of partial differential equations (PDEs) for physical quantities in terms of the spatial coordinates $\mathbf{x}$ and the time t as

$$\mathcal{L}(\mathbf{u}) = 0. \tag{1}$$

Here, $\mathcal{L}$ is a nonlinear operator and $\mathbf{u}(\mathbf{x},t)$ is the vector of dependent variables. When the boundary conditions are somehow simple, approximate variational methods based on modal decomposition and Galerkin's projection[3] can be used to reduce the order of governing equations. These methods begin with solving an auxiliary eigenvalue problem, which is usually the variational field equation $\delta\mathcal{L}(\mathbf{u},\Lambda)=0$, and build some complete basis set $\mathbf{U}_{\mathbf{k}}(\mathbf{x},\Lambda_{\mathbf{k}})$ for expanding $\mathbf{u}(\mathbf{x},t)$ in the spatial domain. Here, $\Lambda_{\mathbf{k}}$ is an *eigenvalue*, which is characterized by the vectorial index $\mathbf{k}$. Each $\mathbf{U}_{\mathbf{k}}$ is called an eigenmode or a shape function. Such a basis set should preferably satisfy boundary conditions and should be orthogonal.

Once a complete basis set is constructed, one may suppose a solution of the form

$$\mathbf{u}(\mathbf{x},t) = \sum_{\mathbf{k}} \mathbf{V}_{\mathbf{k}}(t) \cdot \mathbf{U}_{\mathbf{k}}(\mathbf{x},\Lambda_{\mathbf{k}}). \tag{2}$$

Substituting from (2) into (1) and taking the inner product

$$\int \mathcal{L}(\mathbf{u}) \cdot \mathbf{U}_{\mathbf{k}'}(\mathbf{x})\mathrm{d}\mathbf{x} = 0, \tag{3}$$

leaves us with a system of nonlinear ordinary differential equations (ODEs) for the amplitude functions $\mathbf{V}_{\mathbf{k}}(t)$. The evolution of the reduced ODEs shows the interaction of different modes and their influence on the development of spatiotemporal patterns.

In a series of papers, Raman and Mote[1,4] used the modal decomposition method to investigate transversal oscillations of spinning disks whose deformation field is described in terms of the displacement vector (u,v,w) with u and v being the in-plane components. The most important application of the spinning disk problem is in the design, fabrication, and control of HDDs. The governing PDEs for the evolution of displacement components were first derived by Nowinski[5] and were reformulated more recently by Baddour and Zu.[6] Let us define (R,ϕ) as the usual polar coordinates. For a rotating disk with the angular velocity Ω_0, Nowinski's theory assumes that the in-plane inertias $(u,v)\Omega_0^2$, $2\Omega_0(u_{,t},v_{,t})$, and $(u_{,tt},v_{,tt})$ are ignorable against $R\Omega_0^2$. This is a rough approximation for high-speed disks, and one needs to use the complete set of equations as Baddour and Zu[6] suggest. Nowinski's theory, however, has its own advantages (such as the existence of a stress function) that facilitate the study of the most important transversal modes. In low-speed disks, or

[a]Electronic mail: arzhang_a@mehr.sharif.edu
[b]Electronic mail: mjalali@sharif.edu; URL: http://sharif.edu/~mjalali

disks with high flexural rigidity, one has $\Omega_0 \ll \omega$. Hence, it is legitimate to apply Nowinski's governing equations in such systems.

In this paper, we *analytically prove* the existence of chaos, and therefore, nonintegrability of the reduced ODEs that govern the double-mode oscillations of imperfect spinning disks. We investigate low-speed disks subject to a lateral point force exerted by the magnetic head. The lateral force in HDDs is very small and its origin is the aerodynamic force due to air flow in the gap between the disk and the head. We show that chaotic circumferential waves dominate some zones of the phase space over the time scale $t \sim \mathcal{O}(\epsilon^{-3})$ with ϵ being a small perturbation parameter. This indicates very slow evolution of random patterns, and the practical difficulties of their identification.

The paper is organized as follows. In Sec. II, we present the Hamiltonian function in terms of Deprit's[7] Lissajous variables. In Sec. III, we use a canonical perturbation theory[8,9] to eliminate the fast anomaly l from the Hamiltonian. The action associated with l then becomes an adiabatic invariant. Transversal intersections of destroyed invariant manifolds, and therefore, nonintegrability of the normalized equations, is proved by a second-order Melnikov method in Sec. IV. We present a complete classification of circumferential waves in Sec. V and end the paper with concluding remarks in Sec. VI.

II. PROBLEM FORMULATION

Let us assume $U_m(R)$ as an orthogonal basis set that represents the disk deformation in the radial direction. The index m stands for the number of radial nodes that $U_m(R)$ has. According to Raman and Mote's[1] treatment of imperfect disks, the following choice of the transversal displacement field,

$$w(R,\phi,t) = U_m(R)[x(t)\cos n\phi + y(t)\sin n\phi], \tag{4}$$

reduces Nowinski's governing equations to a system of ODEs for the amplitude functions $x(t)$ and $y(t)$ as

$$\ddot{x} + \lambda^2 x + \epsilon\gamma(x^2+y^2)x = \epsilon F\cos(n\Omega_0 t), \tag{5a}$$

$$\ddot{y} + \omega^2 y + \epsilon\gamma(x^2+y^2)y = \epsilon F\sin(n\Omega_0 t), \tag{5b}$$

where λ, ω, and γ are constant parameters that depend on the geometry and material of the disk. ϵ is a small perturbation parameter, F is the weighted integral of the lateral point force, and Ω_0 is the angular velocity of the disk.

We suppose small deviations from perfect disks and write $\lambda^2/\omega^2 = 1+\epsilon\eta$. We also define $n\Omega_0 = \epsilon\Omega$ with $\mathcal{O}(\Omega) \sim \mathcal{O}(\omega)$. Denoting (p_x, p_y) as the momenta conjugate to (x,y), it can be verified that Eqs. (5) are derivable from the Hamiltonian function

$$H = \frac{1}{2}(p_x^2+p_y^2) + \frac{1}{2}\omega^2(x^2+y^2) + \epsilon\left[\frac{\eta}{2}\omega^2x^2 + \Omega P + \frac{\gamma}{4}(x^2+y^2)^2 - F(x\cos p + y\sin p)\right]. \tag{6}$$

We have introduced the action P and its conjugate angle $p = \epsilon\Omega t$ to make our equations autonomous, which is a preferred form for the application of canonical perturbation theories. The *extended phase space* has now dimension six. Dynamics generated by (6) is better understood after carrying out a canonical transformation $(x,y,p_x,p_y) \to (l,g,L,G)$ to the space of Lissajous variables[7] so that

$$x = s\cos(g+l) - d\cos(g-l), \tag{7a}$$

$$y = s\sin(g+l) - d\sin(g-l), \tag{7b}$$

$$p_x = -\omega[s\sin(g+l) + d\sin(g-l)], \tag{7c}$$

$$p_y = \omega[s\cos(g+l) + d\cos(g-l)], \tag{7d}$$

$$s = \sqrt{\frac{L+G}{2\omega}}, \quad d = \sqrt{\frac{L-G}{2\omega}}, \quad L \geq 0, \quad |G| \leq L.$$

In the space of Lissajous variables, the Hamiltonian defined in (6) becomes

$$H = H_0(L) + \epsilon H_1(l,g,p,L,G,P),$$

$$H_0 = \omega L,$$

$$\begin{aligned} H_1 = {}& \Omega P - F[s\cos(g+l-p) - d\cos(g-l-p)] \\ & + \frac{\gamma}{4}[(s^2+d^2) - 2sd\cos(2l)]^2 \\ & + \frac{\eta\omega^2}{4}[(s^2+d^2) + s^2\cos(2g+2l) - 2sd\cos(2g) \\ & + d^2\cos(2g-2l) - 2sd\cos(2l)]. \end{aligned} \tag{8}$$

From (8) we conclude that l is the fast angle, and g and p are the slow ones. Therefore, the long-term behavior of the flows generated by (8) can be analyzed by averaging H over l. After removing l, its corresponding action L will be a constant of motion for the flows generated by the averaged Hamiltonian $\langle H\rangle_l$, and the phase space dimension reduces from 6 to 4.

III. CANONICAL THIRD-ORDER AVERAGING

In order to average H over l, we use the normalization procedure of Deprit and Elipe.[9] Denoting $X \equiv (l,g,p)$ and $Y \equiv (L,G,P)$, we define a Lie transformation $(l,g,p,L,G,P) \to (\bar{l},\bar{g},\bar{p},\bar{L},\bar{G},\bar{P})$ as

$$X = E_W(\bar{X}), \quad Y = E_W(\bar{Y}), \tag{9}$$

so that the Hamiltonian function in terms of the new variables $K \equiv \langle H\rangle_l$ does not depend on $\bar{l}$. E_W is the Lie transform generated by the function W and it is defined as

$$E_W(\bar{Z}) = \bar{Z} + (\bar{Z};W) + \frac{1}{2!}((\bar{Z};W);W) + \frac{1}{3!}(((\bar{Z};W);W);W) + \cdots . \quad (10)$$

In this equation, $(f_1;f_2)$ denotes the Poisson bracket of f_1 and f_2 over the $(\bar{l},\bar{g},\bar{p},\bar{L},\bar{G},\bar{P})$-space. We expand the generating function W as

$$W = \epsilon W_1 + \frac{\epsilon^2}{2!}W_2 + \cdots , \quad (11)$$

and specify the averaged, *target Hamiltonian* $K = K(\bar{g},\bar{p},\bar{L},\bar{G},\bar{P})$ as the series[9]

$$K = K_0 + \epsilon K_1 + \frac{\epsilon^2}{2!}K_2 + \frac{\epsilon^3}{3!}K_3 + \cdots , \quad (12)$$

with

$$K_0 = \omega \bar{L}, \quad (13a)$$

$$K_1 = \frac{1}{2\pi}\int_0^{2\pi} H_1 \mathrm{d}\bar{l}, \quad (13b)$$

$$K_2 = \frac{1}{2\pi}\int_0^{2\pi} [2(H_1;W_1) + ((H_0;W_1);W_1)]\mathrm{d}\bar{l}, \quad (13c)$$

$$K_3 = \frac{1}{2\pi}\int_0^{2\pi} [3(H_1;W_2) + 3((H_1;W_1);W_1) + 2((H_0;W_2);W_1) + ((H_0;W_1);W_2) + (((H_0;W_1);W_1);W_1))\mathrm{d}\bar{l}. \quad (13d)$$

W_1 and W_2 are determined through solving the following differential equations:

$$\omega\frac{\partial W_1}{\partial \bar{l}} = H_1(\bar{l},\bar{g},\bar{p},\bar{L},\bar{G},\bar{P}) - K_1(\bar{g},\bar{p},\bar{L},\bar{G},\bar{P}), \quad (14a)$$

$$\omega\frac{\partial W_2}{\partial \bar{l}} = 2(H_1;W_1) + ((H_0;W_1);W_1) - K_2. \quad (14b)$$

By substituting (14) into (13) and evaluating the integrals, one finds the explicit form of the new Hamiltonian K, which has been given in Appendix A up to the third-order terms.

Once $\bar{l}$ is removed from the Hamiltonian, $\bar{L}$ becomes an integral of motion. The slow dynamics of the system is thus governed by the flows in the $(\bar{g},\bar{G})$-space. We introduce the *slow time* $\tau = \bar{p}/\Omega$, ignore the fourth-order terms in ϵ, and obtain the following differential equations for the dynamics of $(\bar{g},\bar{G})$:

$$\frac{\mathrm{d}\bar{g}}{\mathrm{d}\tau} = \frac{\partial K}{\partial \bar{G}} = f_1(\bar{g},\bar{G}) + \epsilon h_1(\bar{g},\bar{G},\epsilon,\tau), \quad (15a)$$

$$\frac{\mathrm{d}\bar{G}}{\mathrm{d}\tau} = -\frac{\partial K}{\partial \bar{g}} = f_2(\bar{g},\bar{G}) + \epsilon h_2(\bar{g},\bar{G},\epsilon,\tau), \quad (15b)$$

where

$$f_1 = d_6 + d_1\cos(2\bar{g}), \quad f_2 = e_1\sin(2\bar{g}),$$

$$h_1 = d_7 + d_2\cos(2\bar{g}) + \epsilon[d_8 + d_3\cos(2\bar{g}) + d_4\cos(4\bar{g}) + d_5\cos(2\bar{g} - 2\Omega\tau)], \quad (16)$$

$$h_2 = e_2\sin(2\bar{g}) + \epsilon[e_3\sin(2\bar{g}) + e_4\sin(4\bar{g}) + e_5\sin(2\bar{g} - 2\Omega\tau)].$$

In these equations, d_i $(i=1,\ldots,8)$ and e_j $(j=1,\ldots,5)$ are functions of $\bar{L}$ and $\bar{G}$ (see Appendix A). It is remarked that the action $\bar{P}$ appears only in K_1 via the term $\Omega\bar{P}$. It then disappears in the normalized Eqs. (15) after taking the partial derivatives of K with respect to $\bar{g}$ and $\bar{G}$. The partial derivative of K with respect to $\bar{P}$ determines the evolution of $\bar{p}$, which is in accordance with the simple linear law $\bar{p}(\tau) = \Omega\tau + \bar{p}(0)$. The dynamics of $\bar{P}$ itself is governed by

$$\frac{\mathrm{d}\bar{P}}{\mathrm{d}\tau} = -\frac{\partial K}{\partial \bar{p}} = -\frac{1}{\Omega}\frac{\partial}{\partial \tau}K(\bar{g},\bar{G},\tau). \quad (17)$$

One may integrate (17) to obtain $\bar{P}(\tau)$ once Eqs. (15) are solved. The behavior of $\bar{P}$ is thus inherited from $\bar{g}(\tau)$ and $\bar{G}(\tau)$.

IV. THE MELNIKOV FUNCTION

There are few analytical methods in the literature for the detection of chaos in perturbed Hamiltonian systems.[10,11] Melnikov's[10] method is the most powerful technique when the governing equations take the form

$$\frac{\mathrm{d}\mathbf{x}}{\mathrm{d}\tau} = \mathbf{f}(\mathbf{x}) + \epsilon\mathbf{h}(\mathbf{x},\epsilon,\tau), \quad \mathbf{x} \in \mathbb{R}^2, \quad (18)$$

so that the unperturbed system $\mathrm{d}\mathbf{x}/\mathrm{d}\tau = \mathbf{f}(\mathbf{x})$ is integrable and possesses a homoclinic (heteroclinic) orbit $\mathbf{q}_h(\tau)$ to a hyperbolic saddle point, and $\mathbf{h}(\mathbf{x},\epsilon,\tau)$ is T-periodic in τ. The occurrence of chaos is examined by the Melnikov function

$$M(\tau_0,\epsilon) = \epsilon M_1(\tau_0) + \epsilon^2 M_2(\tau_0) + \cdots , \quad (19)$$

where $M_k(\tau_0)$ denotes the kth-order Melnikov function. Assume that $M_i(\tau_0)$ is the first nonzero term; i.e., $M_k(\tau_0) \equiv 0$ for $1 \leq k \leq i-1$. If $M_i(\tau_0)$ has simple zeros, then, for sufficiently small ϵ, the system (18) has transverse homoclinic (heteroclinic) points, which imply chaos due to the Smale-Birkhoff homoclinic theorem.[12] The first-order term in (19) is determined by the classical formula

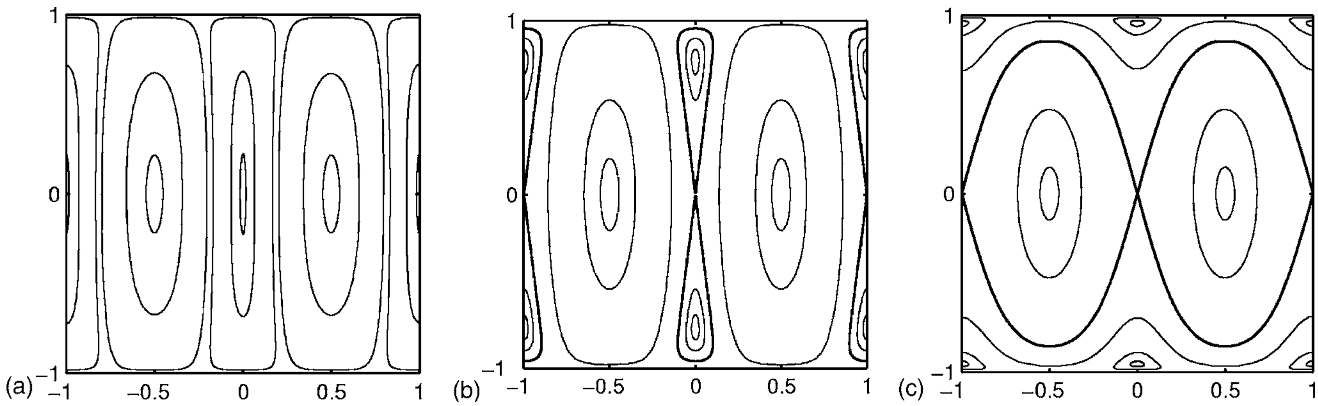

FIG. 1. Possible topologies of the phase space flows of the averaged system for $F=0$. In all panels the horizontal axis indicates $\bar{g}/\pi$ and the vertical axis indicates $\bar{G}/\bar{L}$. In the first topology (left panel), all stationary points are of center type. In the second topology (middle panel) two new centers, with nonzero $\bar{G}$-coordinates, have emerged for $\bar{g}=\pm n\pi$ $(n=0,1)$ and symmetrical homoclinic loops (thick lines) connect saddle points to themselves. In the third topology (right panel) the off-axis centers (and their surrounding tori) are still present, but the separatrix curves (thick lines) are of heteroclinic type.

$$M_1(\tau_0)=\int_{-\infty}^{+\infty}\mathbf{f}[\mathbf{q}_h(\tau)]\wedge\mathbf{h}[\mathbf{q}_h(\tau),0,\tau+\tau_0]\mathrm{d}\tau, \quad (20)$$

where the wedge operator $\wedge$ is defined as $\mathbf{f}\wedge\mathbf{h}=f_1h_2-f_2h_1$. Although the Hamiltonian equations (15) have a suitable form for the application of Melnikov's method, they are autonomous up to the first-order terms in ϵ. Consequently, $M_1(\tau_0)$ vanishes identically for all $\tau_0\in[0,T]$. We thus need to investigate the second-order Melnikov function. To do so, we begin with solving the unperturbed system

$$\frac{\mathrm{d}\bar{g}}{\mathrm{d}\tau}=\frac{\partial K_1}{\partial\bar{G}}=f_1(\bar{g},\bar{G}), \quad (21a)$$

$$\frac{\mathrm{d}\bar{G}}{\mathrm{d}\tau}=-\frac{\partial K_1}{\partial\bar{g}}=f_2(\bar{g},\bar{G}), \quad (21b)$$

along homoclinic (heteroclinic) orbits. Jalali and Angoshtari[2] showed that for $\bar{L}>\eta\omega^3/\gamma$, Eqs. (21) have hyperbolic stationary points at $S_0\equiv(\bar{g}_0,\bar{G}_0)=(-\pi,0)$, $S_2\equiv(\bar{g}_2,\bar{G}_2)=(0,0)$, and $S_4\equiv(\bar{g}_4,\bar{G}_4)=(\pi,0)$. The *implicit* equation of the invariant manifolds that terminate at the saddle points are

$$\cos[2\bar{g}_h(\tau)]=\left[\bar{L}-\frac{\gamma}{2\eta\omega^3}\bar{G}_h^2(\tau)\right][\bar{L}^2-\bar{G}_h^2(\tau)]^{-1/2}. \quad (22)$$

For $\gamma\bar{L}\geq 2\eta\omega^3$, Eq. (22) represents a heteroclinic orbit that connects S_0 to S_2. For $\eta\omega^3<\gamma\bar{L}<2\eta\omega^3$, the heteroclinic orbit disappears and it is replaced by a homoclinic orbit (see Fig. 1). To compute the *explicit* form of the homoclinic (or heteroclinic) orbit of (21), we use (21b) and (22), and obtain

$$\int_{\bar{G}_h(0)}^{\bar{G}_h(\tau)}\frac{\mathrm{d}\bar{G}}{\bar{G}\sqrt{1-\alpha\bar{G}^2}}=\pm\sqrt{\beta}\tau,$$

$$\alpha=\frac{\gamma^2}{16\eta\beta\omega^4},\quad \beta=\frac{\gamma\bar{L}-\eta\omega^3}{4\omega}, \quad (23)$$

where the lower integration limit is $\bar{G}_h(0)=1/\sqrt{\alpha}$. After taking the integral (23), we arrive at

$$\bar{G}_h(\tau)=\frac{\mathrm{sech}(\sqrt{\beta}\tau)}{\sqrt{\alpha}}, \quad (24)$$

for the $\bar{G}\geq 0$ branch of the homoclinic (heteroclinic) orbit. Having $\bar{G}_h(\tau)$, it is straightforward to calculate $\cos[2\bar{g}_h(\tau)]$ and $\sin[2\bar{g}_h(\tau)]$, and to determine the explicit form of $\mathbf{q}_h(\tau)=[\bar{g}_h(\tau),\bar{G}_h(\tau)]$.

For constructing $M_2(\tau_0)$, we use Françoise's[13,14] algorithm that has been devised for dynamical systems with polynomial nonlinearities. To express the averaged Hamiltonian K in terms of polynomial functions of some new dependent variables, we utilize Hopf's variables

$$Q_1=\frac{1}{2\omega}\sqrt{\bar{L}^2-\bar{G}^2}\cos(2\bar{g}), \quad (25a)$$

$$Q_2=\frac{1}{2\omega}\sqrt{\bar{L}^2-\bar{G}^2}\sin(2\bar{g}), \quad (25b)$$

and obtain the following differential 1-form for the evolution of the averaged system

$$\frac{\partial K_1}{\partial Q_1}\mathrm{d}Q_1+\frac{\partial K_1}{\partial Q_2}\mathrm{d}Q_2+\epsilon[(s_1+\epsilon s_2)\mathrm{d}Q_2-(z_1+\epsilon z_2)\mathrm{d}Q_1]=0. \quad (26)$$

Here, the first-order Hamiltonian is

$$K_1(Q_1,Q_2)=\frac{\gamma}{2}(Q_1^2+Q_2^2)-\frac{\eta\omega^2}{2}Q_1+C, \quad (27)$$

and

$$s_1=m_1Q_2, \quad (28a)$$

$$z_1=n_1Q_1+n_6, \quad (28b)$$

$$s_2=m_2(Q_1^2+Q_2^2)Q_2+m_3Q_1Q_2+m_4Q_2+m_5\sin(2\Omega\tau), \quad (28c)$$

$$z_2 = n_2(Q_1^2 + Q_2^2)Q_1 + n_3(3Q_1^2 + Q_2^2) + n_4 Q_1 + n_5 \cos(2\Omega\tau) + n_7. \quad (28d)$$

The constant coefficients C, m_i $(i=1,\ldots,5)$, and n_j $(j=1,\ldots,7)$ have been given in Appendix B. A prerequisite for the application of Françoise's[13] algorithm is that for all polynomial 1-forms D that satisfy the condition

$$\int_{\mathbf{q}_h} D \equiv 0, \quad (29)$$

there must exist polynomials $A(Q_1,Q_2)$ and $r(Q_1,Q_2)$ such that $D=\mathrm{d}A+r\mathrm{d}K_1$. We call this the condition (*) and prove in Appendix C that K_1 satisfies the condition (*).

Françoise's algorithm states that if $M_1(\tau_0)=\cdots=M_{k-1}(\tau_0)\equiv 0$ for some integer $k\geqslant 2$, it follows that

$$M_k(\tau_0) = \int_{\mathbf{q}_h} D_k, \quad (30a)$$

$$D_1 = \delta_1, \quad D_m = \delta_m + \sum_{i+j=m} r_i \delta_j, \quad (30b)$$

$$\delta_j = z_j \mathrm{d}Q_1 - s_j \mathrm{d}Q_2, \quad (30c)$$

for $2\leqslant m\leqslant k$. The functions r_i are then determined successively from the formulas $D_i=\mathrm{d}A_i+r_i\mathrm{d}K_1$ for $i=1,\ldots,k-1$. We have already found that

$$M_1(\tau_0) = \int_{\mathbf{q}_h} \delta_1 = 0, \quad (31)$$

$$\delta_1 = (n_1 Q_1 + n_6)\mathrm{d}Q_1 - m_1 Q_2 \mathrm{d}Q_2. \quad (32)$$

From (30) and (C2a)–(C2d) it can be shown that

$$M_2(\tau_0) = \int_{\mathbf{q}_h} \delta_2. \quad (33)$$

Substituting (30c) and (28) into (33), and carrying out the integration along $\mathbf{q}_h(\tau)$, result in

$$M_2(\tau_0) = \frac{3\gamma F^2 I}{2\omega^6} \sin(2\Omega\tau_0), \quad (34)$$

with I being a constant (see Appendix D). Equation (34) shows that $\tau_n=n\pi/(2\Omega)$ $(n=1,2,\ldots)$ are simple zeros of $M_2(\tau_0)$ so that

$$M_2(\tau_n) = 0, \quad \left.\frac{\partial M_2(\tau_0)}{\partial \tau_0}\right|_{\tau_0=\tau_n} \neq 0. \quad (35)$$

Thus, we conclude that the global stable and unstable manifolds of the saddle point $S_n^{\tau_0}$, $W^s(S_n^{\tau_0})$ and $W^u(S_n^{\tau_0})$, always intersect transversely. Transversal intersections cause a sensitive dependence on initial conditions due to the Smale-Birkhoff homoclinic theorem. This is a route to chaos. On the other hand, this means that the reduced Eqs. (15) are nonintegrable for $F\neq 0$.

V. CLASSIFICATION OF CIRCUMFERENTIAL WAVES

For $F=0$, $\mathbf{h}$ does not depend on τ and the normalized Eqs. (15) are integrable. In such a circumstance, the phase space structure can take three general topologies (depending on the values of the system parameters and $\bar{L}$) as shown in Fig. 1. In the first topology, all stationary points with the coordinates $(\bar{g}_s,\bar{G}_s)$ calculated from

$$\mathbf{f}(\bar{g}_s,\bar{G}_s) + \epsilon\mathbf{h}(\bar{g}_s,\bar{G}_s,\epsilon) = \mathbf{0}, \quad (36)$$

are centers and they lie on the $\bar{G}=0$ axis with $\bar{g}_s=-\pi+n\pi/2$ $(n=0,\ldots,4)$. In the second and third topologies, two off-axis centers (with $\bar{G}_s\neq 0$) come to existence for $\bar{g}_s=\pm n\pi$ $(n=0,1)$ and the on-axis stationary points with the same $\bar{g}_s=\pm n\pi$ become saddles. In the second topology, each saddle point is connected to itself by a homoclinic orbit, and in the third topology, a heteroclinic orbit connects two neighboring saddle points. The system with heteroclinic orbits allows for rotational $\bar{g}(\tau)$, while in the system with homoclinic orbits $\bar{g}(\tau)$ is always librating. Beware that this classification of phase space flows is valid as long as ϵ is sufficiently small.

For $F=0$, the phase space flows of (15) are structurally stable (with no unbounded branches) and the whole $(\bar{g},\bar{G})$-space is occupied by periodic orbits of period $T(K)$. At the stationary points, one has $T[K(\bar{g}_s,\bar{G}_s,\bar{L})]=0$. Given the invariance of $\bar{L}$, and the periodic solutions $\bar{g}(\tau)=\bar{g}[\tau+T(K)]$ and $\bar{G}(\tau)=\bar{G}[\tau+T(K)]$, the anomaly $\bar{l}$ is determined through solving

$$\frac{\mathrm{d}\bar{l}}{\mathrm{d}t} = \omega + \epsilon\frac{\partial}{\partial \bar{L}}\left(K_1 + \frac{\epsilon}{2!}K_2 + \frac{\epsilon^2}{3!}K_3\right), \quad (37)$$

which results in $\bar{l}=\omega t+\epsilon R_l(\tau)$ with $R_l(\tau)=R_l[\tau+T(K)]$. According to (9), the functions $g(t)$, $G(t)$, and $L(t)$ are also periodic in t, and we conclude that $l(t)=\omega t+R_W(t)$ with $R_W(t)=E_W(\bar{l})-\omega t$ being a small-amplitude periodic function of t. The explicit from of the circumferential wave will then become

$$\frac{w(R,\phi,t)}{U_m(R)} = \sqrt{\frac{L(t)+G(t)}{2\omega}}\cos[n\phi-\omega t-R_W(t)-g(t)] - \sqrt{\frac{L(t)-G(t)}{2\omega}}\cos[n\phi+\omega t+R_W(t)-g(t)], \quad (38)$$

which is composed of a forward and a backward traveling wave. Due to the periodic nature of $L(t)$ and $G(t)$, when the amplitude of the forward traveling wave is maximum, that of the backward wave is minimum and vice versa.

As our results of Sec. IV show, the regular nature of traveling waves is destroyed for $F\neq 0$ and a chaotic layer occurs through the destruction of the homoclinic and heteroclinic orbits of (21). This happens over the time scale $\tau\sim\mathcal{O}(\epsilon^{-2})$ or $t\sim\mathcal{O}(\epsilon^{-3})$ (because $\bar{p}$ is present only in K_3). Figure 2 shows Poincaré maps of the system (15) for $F\neq 0$. The sampling time step in generating the Poincaré maps has

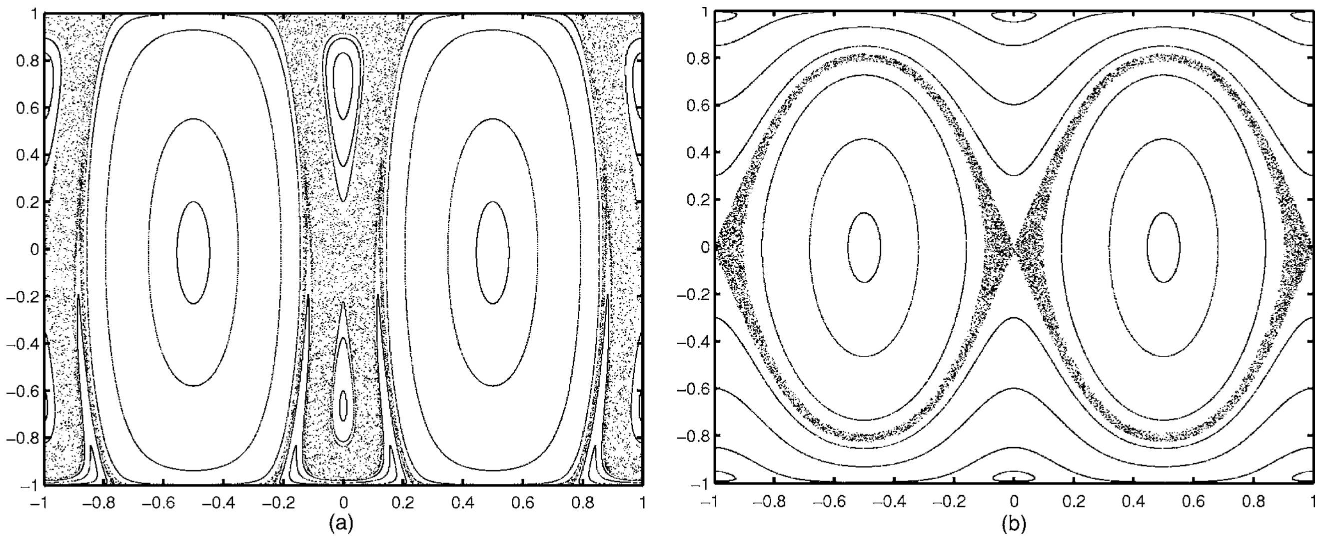

FIG. 2. Phase space structure of the normalized Eqs. (15) with $\bar{L}=2$, $\omega=\eta=F=1$, and $\Omega=\epsilon=0.1$. *Left panel*: $\gamma=0.8$. *Right panel*: $\gamma=2$. In both panels, the horizontal and vertical axes indicate $\bar{g}/\pi$ and $\bar{G}/\bar{L}$, respectively.

been $2\pi/\Omega$. It is seen that most tori around elliptic fixed points are preserved. They correspond to regular periodic and quasiperiodic solutions of the normalized system. For chaotic flows, the functions $\bar{g}(\tau)$ and $\bar{G}(\tau)$ change randomly within the invariant measure of the chaotic set. Consequently, the original Lissajous variables $g(t)$, $L(t)$, $G(t)$, and also $R_W(t)$ become chaotic, too.

For $\bar{G}(\tau)>0$ and $\bar{G}(\tau)<0$ the forward and the backward traveling waves are the dominant components of the circumferential wave, respectively. When the chaotic layer emerges from the destroyed homoclinic orbits (left panel in Fig. 2), the sign of $\bar{G}(\tau)$ is randomly switched along a chaotic trajectory. This means a random transfer of kinetic/potential energy between the forward and backward traveling wave components. For chaotic trajectories of this kind, the angle $\bar{g}(\tau)$ fluctuates randomly near $\bar{g}\approx \pm n\pi$ $(n=0,1)$ with an almost zero average. The evolution of circumferential waves is quite different when the chaotic layer emerges due to destroyed heteroclinic orbits (right panel in Fig. 2). In this case, chaos means a random change between the librational and rotational states of $\bar{g}(\tau)$. Such a change induces an unpredictable phase shift of magnitude π for both forward and backward traveling wave components. We note that $\bar{G}(\tau)$ can flip sign on a chaotic trajectory only when $\bar{g}(\tau)$ is in its librational state.

VI. CONCLUDING REMARKS

Resonance overlapping[11,16] is the main cause for chaotic behavior in spinning disks with near-resonant angular velocities.[1,2] The chaos predicted in this paper, however, happens far from fundamental resonances. Optical drives and HHDs are usually operated below critical resonant speeds and the lateral force F due to magnetic head is very small. We showed that whatever the magnitude of F may be, a chaotic layer fills some parts of the phase space because the Melnikov function of the normalized equations has *always* simple zeros. Dynamics of rotating disks is regular only if F vanishes, which is an unrealistic assumption for disk drives. In low-speed disks with small F, diffusion of chaotic orbits (within their invariant measure) takes a long time of $t\sim\mathcal{O}(\epsilon^{-3})$. The slow development of chaotic circumferential waves makes them undetectable in short time scales at which most controllers work. The Melnikov function (34) depends not only on F, but also on the parameter η through the constant I. The parameter η is a contribution of imperfections, which are likely because of limited fabrication precision in micro/nano scales. For a perfect disk with $\eta=0$, the off-axis elliptic stationary points of (21), and consequently, homoclinic and heteroclinic orbits disappear. In such a condition the Melnikov function is indefinite, but the system admits an exact first integral and the dynamics is governed by the Hamiltonian function given in Eq. (11) of Jalali and Angoshtari.[2]

One of the most important achievements of this work was to unveil the fact that it is premature to truncate the series of canonical perturbation theories before recording the role of all participating variables. In systems with nonautonomous governing ODEs (nonconservative systems), one must be cautious while removing a fast angle through averaging schemes. The removal of the fast angle may also wipe out time-dependent terms, up to some finite orders of ϵ, and hide some essential information of the underlying dynamical process. Strange, irregular solutions can indeed occur at any order and influence the long-term response of dynamical systems, as we observed for the spinning disk problem by keeping the third-order terms.

ACKNOWLEDGMENTS

We are indebted to the anonymous referee who discovered an error in the early version of the paper and led us to investigate the second-order Melnikov function. M.A.J. thanks the Research Vice-Presidency at Sharif University of Technology for partial support.

APPENDIX A: THE NORMALIZED HAMILTONIAN

By evaluating the integrals in (13), we obtain the first-, second-, and third-order terms of the normalized Hamiltonian as

$$K_1 = \frac{-\gamma\bar{G}^2}{8\omega^2} + \frac{\bar{L}(3\gamma\bar{L}+2\eta\omega^3)}{8\omega^2} + \Omega\bar{P} - \frac{\eta\omega}{4}\sqrt{\bar{L}^2-\bar{G}^2}\cos(2\bar{g}), \quad \text{(A1)}$$

$$K_2 = -\frac{1}{64\omega^5}[2\bar{L}(-9\bar{G}^2+17\bar{L}^2)\gamma^2 + 64F^2\omega^3 + 8(3\bar{L}^2-\bar{G}^2)\gamma\eta\omega^3 + 8\bar{L}\eta^2\omega^6 + 4\omega^3[-6\bar{L}\gamma\eta - 2\eta^2\omega^3]\sqrt{\bar{L}^2-\bar{G}^2}\cos(2\bar{g})], \quad \text{(A2)}$$

$$K_3 = \frac{3}{512\omega^8}\{11\bar{G}^4\gamma^3 - 258\bar{G}^2\bar{L}^2\gamma^3 + 375\bar{L}^4\gamma^3 + 1024F^2\bar{L}\gamma\omega^3 - 180\bar{G}^2\bar{L}\gamma^2\eta\omega^3 + 340\bar{L}^3\gamma^2\eta\omega^3 + 256F^2\eta\omega^6 - 48\bar{G}^2\gamma\eta^2\omega^6 + 176\bar{L}^2\gamma\eta^2\omega^6 + 32\bar{L}\eta^3\omega^9 - 2\omega^3[17(10\bar{L}^2-\bar{G}^2)\gamma^2\eta + 96\bar{L}\gamma\eta^2\omega^3 + 16\eta^3\omega^6]\sqrt{\bar{L}^2-\bar{G}^2}\cos(2\bar{g}) - 16(\bar{G}^2 - \bar{L}^2)\gamma\eta^2\omega^6\cos(4\bar{g}) + 256F^2\eta\omega^6\cos(2\bar{p}) - 512F^2\gamma\omega^3\sqrt{\bar{L}^2-\bar{G}^2}\cos(2\bar{g}-2\bar{p})\}. \quad \text{(A3)}$$

Consequently, the functions $d_i(\bar{L},\bar{G})$ in Eqs. (16) are found to be

$$d_1 = \frac{\eta\omega\bar{G}}{4}(\bar{L}^2-\bar{G}^2)^{-1/2},$$

$$d_2 = -\frac{\bar{G}}{16\omega^2}(6\bar{L}\gamma\eta + 2\eta^2\omega^3)(\bar{L}^2-\bar{G}^2)^{-1/2},$$

$$d_3 = \frac{3\bar{G}}{256\omega^5}[16\eta^3\omega^6 + 51(4\bar{L}^2-\bar{G}^2)\gamma^2\eta + 96\bar{L}\gamma\eta^2\omega^3](\bar{L}^2-\bar{G}^2)^{-1/2},$$

$$d_4 = -\frac{3\bar{G}\gamma\eta^2}{16\omega^2}, \quad \text{(A4)}$$

$$d_5 = \frac{3\bar{G}F^2\gamma}{\omega^5}(\bar{L}^2-\bar{G}^2)^{-1/2},$$

$$d_6 = -\frac{\gamma\bar{G}}{4\omega^2},$$

$$d_7 = \frac{\bar{G}}{32\omega^5}(18\bar{L}\gamma^2 + 8\gamma\eta\omega^3),$$

$$d_8 = \frac{3\bar{G}}{256\omega^8}[2\gamma^3(11\bar{G}^2 - 129\bar{L}^2) - 180\bar{L}\gamma^2\eta\omega^3 - 48\gamma\eta^2\omega^6].$$

Defining $S=(\bar{L}^2-\bar{G}^2)/\bar{G}$, the functions $e_j(\bar{L},\bar{G})$ in Eqs. (16) become

$$e_j = -2d_jS, \quad j=1,\ldots,5, \quad j\neq 3,$$

$$e_3 = -\frac{3}{128\omega^5}[16\eta^3\omega^6 + 17(10\bar{L}^2-\bar{G}^2)\gamma^2\eta + 96\bar{L}\gamma\eta^2\omega^3]\sqrt{\bar{L}^2-\bar{G}^2}. \quad \text{(A5)}$$

APPENDIX B: THE COEFFICIENTS OF THE DIFFERENTIAL 1-FORM

The constant coefficients of Eqs. (27) and (28) are as follows:

$$C = \frac{\bar{L}(\gamma\bar{L}+\eta\omega^3)}{4\omega^2},$$

$$n_1 = \frac{1}{8\omega^3}(9\bar{L}\gamma^2 + 4\gamma\eta\omega^3),$$

$$n_2 = -\frac{33\gamma^3}{48\omega^4},$$

$$n_3 = \frac{17\gamma^2\eta}{64\omega^2},$$

$$n_4 = -\frac{1}{32\omega^6}(59\bar{L}^2\gamma^3 + 45\bar{L}\gamma^2\eta\omega^3 + 16\gamma\eta^2\omega^6),$$

$$n_5 = \frac{F^2\gamma}{\omega^4}, \quad \text{(B1)}$$

$$n_6 = -\frac{3\bar{L}\gamma\eta + \eta^2\omega^3}{8\omega},$$

$$n_7 = \frac{1}{256\omega^4}(153\bar{L}^2\gamma^2\eta + 96\bar{L}\gamma\eta^2\omega^3 + 16\eta^3\omega^6),$$

$$m_i = -n_i, \quad i=1,\ 2,\ 5,$$

$$m_3 = -2n_3,$$

$$m_4 = \frac{1}{32\omega^6}(59\bar{L}^2\gamma^3 + 45\bar{L}\gamma^2\eta\omega^3 + 8\gamma\eta^2\omega^6).$$

APPENDIX C: THE CONDITION (*)

In this appendix we prove that $K_1(Q_1,Q_2)$ given in (27) satisfies the condition (*). To this end, we need the following theorem.

Theorem 1. *Any polynomial 1-form D of degree n in Q_1*

and Q_2 can be expressed as

$$D = \mathrm{d}A + r\mathrm{d}K_1 + \xi(K_1)Q_2\mathrm{d}Q_1, \tag{C1}$$

where $A(Q_1,Q_2)$ and $r(Q_1,Q_2)$ are polynomials of degree $(n+1)$ and $(n-1)$, respectively, and $\xi(K_1)$ is a polynomial of degree $\left[\frac{1}{2}(n-1)\right]$, where $[x]$ denotes the greatest integer in x.

Iliev[15] has proved the same theorem for $H=(Q_1^2+Q_2^2)/2$. Theorem 1 can thus be proved in a similar manner. Here we only present a useful result.

Let D be a general polynomial 1-form of degree 1,

$$D = (a_{10}Q_1 + a_{01}Q_2 + a_{00})\mathrm{d}Q_1 + (b_{10}Q_1 + b_{01}Q_2 + b_{00})\mathrm{d}Q_2; \tag{C2a}$$

then in (C1) we have

$$A(Q_1,Q_2) = \frac{a_{10}}{2}Q_1^2 + b_{10}Q_1Q_2 + \frac{b_{01}}{2}Q_2^2 + a_{00}Q_1 + b_{00}Q_2, \tag{C2b}$$

$$r(Q_1,Q_2) = 0, \tag{C2c}$$

$$\xi(K_1) = a_{01} - b_{10}. \tag{C2d}$$

Since $\mathrm{d}K_1=0$ along any phase space orbit characterized by $K_1(Q_1,Q_2)=k$, and since the integral of an exact differential $\mathrm{d}A$ around any closed curve is zero, from (C1) we obtain

$$\int_{\mathbf{q}_h} D = \xi(k)\int_{\mathbf{q}_h} Q_2\mathrm{d}Q_1 = \xi(k)\int_{-\infty}^{+\infty} Q_2(\tau)\frac{\mathrm{d}Q_1}{\mathrm{d}\tau}\mathrm{d}\tau.$$

On the other hand, from (25a) we have

$$\frac{\mathrm{d}Q_1}{\mathrm{d}\tau} = E(\tau) - 2Q_2,$$

where $E(\tau)$ is an even function of τ. Given the fact that Q_2 is an odd function of τ, we conclude that

$$\int_{\mathbf{q}_h} D = -2\xi(k)\int_{-\infty}^{+\infty} Q_2^2\mathrm{d}\tau.$$

Consequently, if $\int_{\mathbf{q}_h} D \equiv 0$, it follows that $\xi(k)\equiv 0$, and therefore $D=\mathrm{d}A+r\mathrm{d}K_1$, which completes the proof. □

APPENDIX D: THE COEFFICIENT I IN $M_2(\tau_0)$

In Eq. (34), the constant coefficient I is

$$\begin{aligned} I = &-\frac{64\pi\sqrt{\eta}\Omega^2\omega^2}{\gamma}\,\mathrm{csch}\left(\frac{\pi\Omega}{\sqrt{\beta}}\right) \\ &+ \frac{\pi\omega\sqrt{\eta}(3\gamma\bar{L} - 4\eta\omega^3)(\beta+4\Omega^2)}{\gamma\beta}\,\mathrm{sech}\left(\frac{\pi\Omega}{\sqrt{\beta}}\right) \\ &- \frac{\pi\omega\bar{L}\sqrt{\eta}(3\beta-4\Omega^2)}{\beta}\,\mathrm{sech}\left(\frac{\pi\Omega}{\sqrt{\beta}}\right) \\ &+ \frac{4\pi\eta^{3/2}\omega^4}{\gamma}\,\mathrm{sech}\left(\frac{\pi\Omega}{\sqrt{\beta}}\right). \end{aligned}$$

[1] A. Raman and C. D. Mote Jr., Int. J. Non-Linear Mech. **36**, 261 (2001).
[2] M. A. Jalali and A. Angoshtari, Int. J. Non-Linear Mech. **41**, 726 (2006).
[3] J. N. Reddy, *Applied Functional Analysis and Variational Methods in Engineering* (McGraw-Hill, New York, 1986).
[4] A. Raman and C. D. Mote Jr., Int. J. Non-Linear Mech. **34**, 139 (1999).
[5] J. Nowinski, ASME J. Appl. Mech. **31**, 72 (1964).
[6] N. Baddour and J. W. Zu, Appl. Math. Model. **25**, 541 (2001).
[7] A. Deprit, Celest. Mech. Dyn. Astron. **51**, 201 (1991).
[8] A. Deprit, Celest. Mech. **1**, 12 (1969).
[9] A. Deprit and A. Elipe, Celest. Mech. Dyn. Astron. **51**, 227 (1991).
[10] V. K. Melnikov, Trans. Mosc. Math. Soc. **12**, 1 (1963).
[11] B. V. Chirikov, Phys. Rep. **52**, 263 (1979).
[12] J. Guckenheimer and P. Holmes, *Nonlinear Oscillations, Dynamical Systems, and Bifurcations of Vector Fields* (Springer, New York, 1983).
[13] J. P. Françoise, Ergod. Theory Dyn. Syst. **16**, 87 (1996).
[14] L. Perko, *Differential Equations and Dynamical Systems*, 3rd ed. (Springer, New York, 2001).
[15] I. D. Iliev, Math. Proc. Cambridge Philos. Soc. **127**, 317 (1999).
[16] G. Contopoulos, *Order and Chaos in Dynamical Astronomy* (Springer, New York, 2002).